Accurate time propagation method for the coupled Maxwell and Kohn-Sham equations

Yonghui Li, Shenglai He, Arthur Russakoff, and Kálmán Varga

Phys. Rev. E **94**, 023314 — Published 22 August 2016

DOI: 10.1103/PhysRevE.94.023314

Accurate Time Propagation Method for the Coupled Maxwell and Kohn-Sham Equations

Yonghui Li

Department of Physics and Astronomy,

Vanderbilt University, Nashville, Tennessee, 37235, USA and

Department of Physics, Tianjin University, Tianjin 300072, China

Shenglai He, Arthur Russakoff, and Kálmán Varga*

Department of Physics and Astronomy,

Vanderbilt University, Nashville, Tennessee, 37235, USA

Abstract

An accurate method for time propagation of the coupled Maxwell and time-dependent Kohn-Sham (TDKS) equation is presented. The new approach uses a simultaneous fourth-order Runge-Kutta based propagation of the vector potential and the Kohn-Sham orbitals. The approach is compared to the conventional fourth-order Taylor propagation and predictor-corrector methods. The calculations show several computational and numerical advantages including higher computational performance, greater stability, better accuracy and faster convergence.

* kalman.varga@vanderbilt.edu

I. INTRODUCTION

An accurate description of the interaction of electromagnetic fields and matter is an indispensable tool for understanding and predicting electric and optical properties of nanostructures. Modeling and simulation of this interaction plays a critical role in the foundation of modern electronics, information processing, and optical communications [1–5]. Quantum electrodynamics would, in principle, provide a complete description of these systems, but the high complexity and prohibitively large computational expense prevents its application to realistic systems. A viable alternative is the combination of nonrelativistic quantum mechanics to describe the particles and a classical treatment of the electromagnetic fields. In this semiclassical framework the electromagnetic fields are not quantized and their time evolution is governed by the Maxwell equations coupled to the quantum mechanically determined charge and current distributions of particles [6–8]. A full many-body quantum approach is not tractable for systems containing more then a few electrons, and most approaches are based on the time dependent density functional theory (TDDFT) [9, 10].

Various approaches have been developed to use the coupled Schrödinger and Maxwell systems [6, 8, 11–22]. In problems where the propagation of electromagnetic waves in materials is tackled, most approaches use a finite-difference time-domain solution for the electromagnetic waves and time evolution of the Schrödinger equation in real space for the electrons [19, 21]. Due to the large wavelength of the electromagnetic waves typically considered, the simulation cell has to be large and the atomistic details are suppressed. Yabana et al. [23] devised a multiscale approach where the Maxwell equations are solved on the scale of the electromagnetic wavelength and the Schrödinger equation is solved on the atomic scale using TDDFT. This approach, however, is computationally expensive and only works for certain geometries. At the same time, many problems require the treatment of the electromagnetic fields coupled to the electronic structure at the atomic scale. In this case the electromagnetic fields and the Schrödinger equation is propagated on the same time and length scale [24] which limits the applicability of this method to small simulation cells and short timescales.

In this paper we investigate the simultaneous time propagation of the vector potential of the electromagnetic fields and the wave function describing the electrons of the system. First, we compare the accuracy and efficiency of the conventional approaches [25, 26], then we propose a new method, based on a dual Runge-Kutta approach to improve the time propagation scheme. This approach allows larger time steps and lower computational cost than previously considered

propagators. We use the formalism proposed by Bertsch et al. [24]. In this approach, which has been successfully applied to various problems [23, 25–27], the time-dependent Kohn-Sham equations of TDDFT and Maxwell equations are solved on a real space grid with periodic boundary conditions. To incorporate the electromagnetic fields, the Kohn-Sham equation is coupled to the Maxwell equations by adding a vector potential $\mathrm{A}(t)$ to the linear momentum in the Kohn-Sham equation.

The plan for this paper is as follows. In section II we present the Maxwell-TDKS formalism and the numerical approach used. In section III we review the Taylor and predictor-corrector real-time propagation schemes. In section IV we describe the proposed simultaneous fourth-order Runge-Kutta propagation method and in section V we compare the three propagation schemes. In section VI we summarize the results and conclude this paper.

II. MAXWELL-TDKS EQUATION WITH PERIODIC BOUNDARY CONDITIONS

In systems with the periodic boundary conditions the Kohn-Sham orbitals take the form of Bloch waves,

$$\psi_{ik}(\vec{r},t) = e^{i\vec{k}\cdot\vec{r}}u_{ik}(\vec{r},t), \tag{1}$$

with a lattice periodic spatial part, $u_{ik}(\vec{r},t)$, where i is the orbital and k is the k-vector index, and a phase factor, $e^{i\vec{k}\cdot\vec{r}}$. The Maxwell-TDKS equations can be written as,

$$i\frac{\partial}{\partial t}u_{ik}(\vec{r}\,,t) = H_{KS}(t)u_{ik}(\vec{r},t). \tag{2}$$

The Kohn-Sham Hamiltonian, in atomic units, is given by,

$$\begin{aligned} H_{KS}(t)u_{ik}(\vec{r}\,,t) = &\left[\frac{1}{2}\left(-i\nabla + \vec{k} + \vec{A}(\vec{r},t)\right)^2 + V_{Hxc}[n(\vec{r},t)](\vec{r},t)\right]u_{ik}(\vec{r},t) \\ &+ \int d^3\vec{r}\,' e^{-i(\vec{k}\cdot\vec{r})}v_{pp}(\vec{r}\,,\vec{r}\,')e^{i(\vec{k}\cdot\vec{r}\,')}u_{ik}(\vec{r}\,',t), \end{aligned} \tag{3}$$

where, $n(\vec{r},t)$ is the electron density, $\vec{A}$ is the vector potential, V_{Hxc} is the sum of the Hartree and exchange-correlation potentials, and v_{pp} is the sum of Troullier-Martins [28] norm-conserving pseudopotentials for the ions. The time-dependent density, $n(\vec{r},t)$, is defined as

$$n(\vec{r},t) = 2\sum_{ik}|u_{ik}(\vec{r}\,,t)|^2.$$

The Hartree potential is given by,

$$V_{\text{Hartree}} = \int \frac{n(\vec{r}\,',t)}{|\vec{r}-\vec{r}\,'|}d\vec{r}\,'. \tag{4}$$

The exchange-correlation potential is approximated using the adiabatic local density approximation (ALDA) with the parameterization of Perdew and Zunger [29]. The vector potential, $\vec{A} = \vec{A}_{ext} + \vec{A}_{ind}$, is a "macroscopic" quantity which is the sum of the external field, $\vec{A}_{ext}$, and the induced internal field, $\vec{A}_{ind}$. V_{Hxc} is a "microscopic" field within the unit cell.

Unlike the ordinary TDKS equations, where v_{Hxc} is the only term which depends on the time-dependent density, the vector potential in the Maxwell-TDKS equations also couples to the spatial average of the current density,

$$\frac{\partial^2 \vec{A}}{\partial t^2} = -4\pi \vec{J} = -\frac{4\pi}{\Omega} \int d\vec{r} \left[\vec{j}(\vec{r},t) + \vec{j}_{pp}(\vec{r},t) \right], \tag{5}$$

where $\vec{j}(\vec{r},t)$ is the normal probability current in quantum mechanics while $\vec{j}_{pp}(\vec{r},t)$ is the contribution from the non-local part of the pseudopotential as defined e.g. in [26]. Eq. (5) is the Maxwell-equation describing the time-dependent macroscopic fields induced by the time-dependent currents.

A brief description of the numerical approach is as follows. A real space grid representation [24, 30, 31] is used to solve the TDKS equations, eq. (2). The kinetic energy operator is calculated using a fourth order finite-difference formula. Our test system is a diamond crystal, the same system as used by Bertsch et al. [24]. There are 8 carbon atoms in a cubic box of $L^3 = 6.73^3$ Bohr^3. The grid spacing is $\Delta x = \Delta y = \Delta z = 0.42$ Bohr. An equidistant $2 \times 2 \times 2$ and $5 \times 5 \times 5$ k-point meshes are used. While these meshes may be too small for calculations that can be compared experiments, these k point grids are sufficient for the test of different approaches.

At the beginning of the calculation, the ground-state Kohn-Sham orbitals of the unperturbed system are obtained by solving the time-independent Kohn-Sham equations of density functional theory (DFT). Next the system is perturbed by an instantaneous electric field, $\vec{E}(t)$, in a form of a delta-function kick at time, $t = 0$,

$$\vec{E}(t) = -\frac{d\vec{A}_{ext}}{dt} = -A_0 \delta(t) \vec{e}_z, \tag{6}$$

where $A_0 = 0.01$ a.u. is the strength of the perturbation and $\vec{e}_z$ is the unit vector pointing to the z direction. This gives an initial condition for the vector potential,

$$\vec{A}(t=0) = A_0 \vec{e}_z.$$

The Kohn-Sham orbitals are then propagated in real time. In this paper we consider three propagation algorithms: fourth-order Taylor propagation (Algorithm 1), predictor-corrector (PC) (Algorithm 2), and simultaneous fourth-order Runge-Kutta (SRK4) (Algorithm 3).

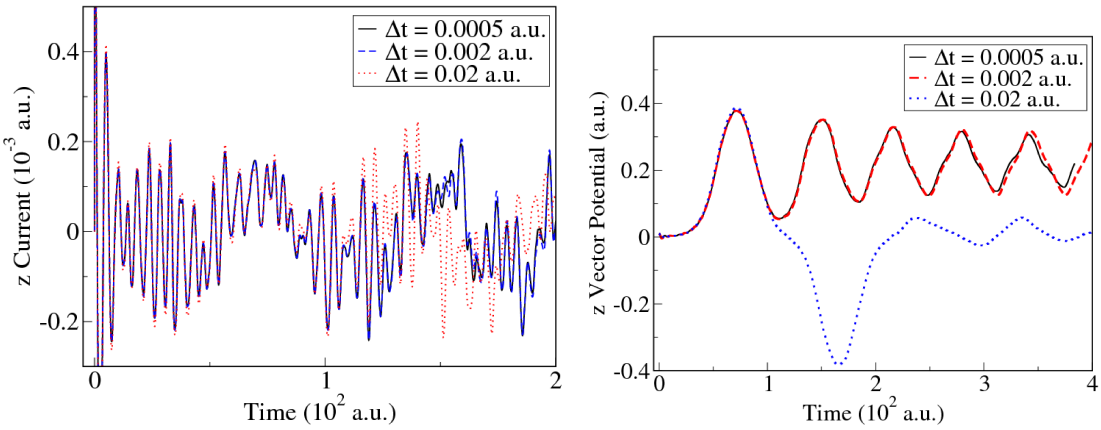

(a) (b)

FIG. 1. (Color online) (a) Current and (b) vector potential in the z direction in a diamond crystal induced by a delta kick applied in the z direction. A $2 \times 2 \times 2$ k-point mesh is used. The Kohn-Sham orbitals are propagated with the Taylor propagation scheme (Algorithm 1) for times up to 400 a.u. Current plotted only up to 200 a.u. Well converged results are obtained for time steps $\Delta t \leq 0.002$ a.u.

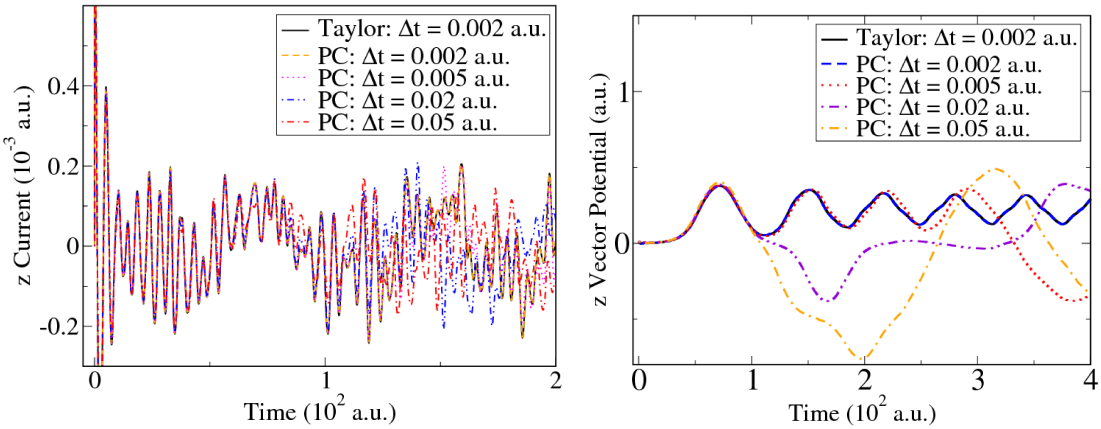

(a) (b)

FIG. 2. (Color online) (a) Current and (b) vector potential in the z direction in a diamond crystal induced by a delta kick applied in the z direction. A $2 \times 2 \times 2$ k-point mesh is used. The Kohn-Sham orbitals are propagated with the predictor-corrector propagation scheme (Algorithm 2) for times up to 400 a.u. Current plotted only up to 200 a.u. The propagation only remains stable for very small time steps, $\Delta t \leq 0.002$ a.u., with the Taylor benchmark and PC method exactly overlapping.

III. TIME PROPAGATION OF THE MAXWELL-TDKS EQUATION

In the fourth-order Taylor propagation, the Kohn-Sham orbitals are propagated as,

$$u_{ik}(\vec{r}, t + \Delta t) = \sum_{n=0}^{4} \frac{1}{n!} \left(-\frac{i\Delta t}{\hbar} H_{KS}(t) \right)^n u_{ik}(\vec{r}, t). \tag{7}$$

This is a conditionally stable propagation scheme. It has proved to be very accurate in many applications [32–42] provided that the time step is sufficiently small.

If one propagates the Kohn-Sham orbitals using the Taylor approach but without including the induced vector potential, the largest time step one may use to obtain well converged results is $\Delta t_0 = 0.04$ a.u. (0.001 fs). V_{Hxc} is a slowly changing quantity which can be treated as a constant during each step of the propagation. In this case the most expensive operation of the calculation is the application of the Kohn-Sham Hamiltonian to the Kohn-Sham orbitals. The commonly used fourth-order Taylor propagator requires four of these sparse matrix-vector operations per Kohn-Sham orbital.

To include the induced current and vector potential, one must propagate the Maxwell-TDKS equations simultaneously. We begin by investigating the simple propagation algorithm shown in Algorithm 1. In this algorithm the Kohn-Sham orbitals are time developed using Taylor propagation and the vector potential is updated using a finite-difference representation of the second derivative. Since the second derivative of the vector potential is related to the current (see eq. (5)), the vector potential is very sensitive to small changes in current. This makes the simultaneous solution of the TDKS and Maxwell-equations more challenging. The induced vector potential changes more rapidly than V_{Hxc}. If a time step on the same order as $\Delta t_0 = 0.04$ a.u. is applied to the Maxwell-TDKS equations using Algorithm 1, the calculation diverges. For example, a time step of $\Delta t_T = 0.02$ a.u. leads to a divergence at 100 a.u. (2 fs) as shown in Fig. 1. Reducing the time step to $\Delta t_T = 0.002$ a.u. gives well converged results. However, this time step is computationally prohibitively expensive (see Table I). Fig. 1 shows that the divergence does not occur at the beginning of the calculation. This makes it difficult to select a proper time step for the Taylor propagator.

Algorithm 1 Taylor Method for the Maxwell-TDKS equation

procedure TAYLOR1STEP($n(\vec{r},t)$, $\{\psi_{ik}(\vec{r},t)\}$, $\vec{A}(t)$, $\vec{A}(t-\Delta t)$) ▷ The initial condition

$V_{Hxc}(\vec{r}) \leftarrow$ COMPUTEVHXC($n(\vec{r},t)$)

$\{\psi_{ik}(\vec{r},t+\Delta t)\} \leftarrow$ TAYLORPROPAGATOR1STEP($\{\psi_{ik}(\vec{r},t)\}$, $\vec{A}(t)$, $V_{Hxc}(\vec{r})$) ▷ 4th order expansion

$\vec{J} \leftarrow$ COMPUTECURRENT($\{\psi_{ik}^{pred}(\vec{r})\}$)

$\vec{A}(t+\Delta t) \leftarrow 2\vec{A}(t) - \vec{A}(t-\Delta t) + (-4\pi)\vec{J}\Delta t^2$

end procedure

To alleviate this problem, the PC method was introduced and has been used in many applications [24, 25, 43]. The PC algorithm is summarized in Algorithm 2. A typical PC method requires two Taylor propagations, and hence 8 applications of the Hamiltonian to each Kohn-Sham orbital.

We use the well converged result of Algorithm 1 with $\Delta t_T = 0.002$ a.u. as a benchmark calculation. In Fig. 2, we calculate the current density and induced vector potential using the PC method and compare to the benchmark. We have found that a time step of $\Delta t_{PC} = 0.005$ a.u. yields a stable propagation within 200 a.u. (5 fs). With larger time steps the results diverge more quickly.

Algorithm 2 PC Method with Taylor Propagator

procedure PREDICTORCORRECTOR1STEP($n(\vec{r},t)$, $\{\psi_{ik}(\vec{r},t)\}$, $\vec{A}(t)$, $\vec{A}(t-\Delta t)$) ▷ The initial condition

$V_{Hxc}(\vec{r}) \leftarrow$ COMPUTEVHXC($n(\vec{r},t)$) ▷ predict stage

$\{\psi_{ik}^{pred}(\vec{r})\} \leftarrow$ TAYLORPROPAGATOR1STEP($\{\psi_{ik}(\vec{r},t)\}$, $\vec{A}(t)$, $V_{Hxc}(\vec{r})$)

$n^{pred}(\vec{r}) \leftarrow$ COMPUTEDENSITY($\{\psi_{ik}^{pred}(\vec{r})\}$)

$V_{Hxc}^{pred}(\vec{r}) \leftarrow$ COMPUTEVHXC($n^{pred}(\vec{r})$)

$\vec{J} \leftarrow$ COMPUTECURRENT($\{\psi_{ik}^{pred}(\vec{r})\}$)

$\vec{A}^{pred} \leftarrow 2\vec{A}(t) - \vec{A}(t-\Delta t) + (-4\pi)\vec{J}\Delta t^2$

$V_{Hxc}^{corr}(\vec{r}) \leftarrow \frac{1}{2}(V_{Hxc}^{pred} + V_{Hxc})$ ▷ correct stage

$\vec{A}^{corr} \leftarrow \frac{1}{2}(\vec{A}^{pred} + \vec{A}(t))$

$\{\psi_{ik}(\vec{r},t+\Delta t)\} \leftarrow$ TAYLORPROPAGATOR1STEP($\{\psi_{ik}(\vec{r},t)\}$, $\vec{A}^{corr}$, $V_{Hxc}^{corr}(\vec{r})$) ▷ real propagation

$n(\vec{r},t+\Delta t) \leftarrow$ COMPUTEDENSITY($\{\psi_{ik}(\vec{r},t+\Delta t)\}$)

$\vec{J} \leftarrow$ COMPUTECURRENT($\{\psi_{ik}(\vec{r},t+\Delta t)\}$)

$\vec{A}(t+\Delta t) \leftarrow 2\vec{A}(t) - \vec{A}(t-\Delta t) + (-4\pi)\vec{J}\Delta t^2$

end procedure

IV. SIMULTANEOUS RUNGE-KUTTA TIME PROPAGATION

While the PC method is a popular approach, it is neither a standard "multi-step" or a "multi-value" differential equation solver [44]. As shown in the previous section, when the induced vector potential is included the PC method leads to numerical instabilities unless a very small time step is used. We propose a Runge-Kutta (RK) based approach as a new propagation method. Compared to the PC method, the RK approach allows for stable propagation with larger time steps and less computational cost per time step.

For convenience we begin by rewriting the Maxwell-TDKS equations as first-order differential equations in time,

$$\frac{\partial u_{ik}(\vec{r},t)}{\partial t} = -iH_{KS}(t)u_{ik}(\vec{r},t) \tag{8}$$

$$\frac{d\dot{\vec{A}}(t)}{dt} = -4\pi\vec{J}, \tag{9}$$

where $\dot{\vec{A}}(t)$ is the first-order time derivative of the vector potential $\vec{A}(t)$. With both equations in the form,

$$\frac{dy}{dt} = f(t, y),$$

one may use the fourth-order Runge-Kutta method (RK4) propagate ψ_{ik} and $\dot{\vec{A}}$ simultaneously. The Runge-Kutta method updates the equations as follows [44]:

$$y(t + \Delta t) = y(t) + \frac{\Delta t}{6}(k_1 + k_2 + k_3 + k_4),$$

where,

$$\begin{aligned}
k_1 &= f(t, y(t)) \\
k_2 &= f(t + \frac{\Delta t}{2}, y(t) + k_1 \frac{\Delta t}{2}) \\
k_3 &= f(t + \frac{\Delta t}{2}, y(t) + k_2 \frac{\Delta t}{2}) \\
k_4 &= f(t + \Delta t, y(t) + k_3 \Delta t).
\end{aligned}$$

By substituting the density, the vector potential and the wave functions, one evaluates the time derivative of the wave functions; one also evaluates the derivative of $\dot{\vec{A}}$ with the averaged current calculated out of the wave functions. The two derivatives can be used to construct the RK4 algorithm.

The simultaneous RK4 (SRK4) algorithm provides $\psi_{ik}(\vec{r}, t + \Delta t)$ and $\dot{\vec{A}}(t + \Delta t)$, but not the vector potential directly. The last piece of the algorithm is the calculation of the vector potential. One possibility for evaluation of the vector potential is a simple finite-difference formula,

$$\vec{A}(t + \Delta t) \approx 2\vec{A}(t) - \vec{A}(t - \Delta t) + \Delta t^2 \, \ddot{\vec{A}}(t), \tag{10}$$

as it has been used in Algorithms 1 and 2, but this implementation uses two previous time steps. Considering that the RK4 algorithm is the algorithm depends only on the previous step, the Euler method is a more suitable approach.

$$\vec{A}(t + \Delta t) \approx \vec{A}(t) + \Delta t \, \dot{\vec{A}}(t). \tag{11}$$

To obtain the same order of accuracy as eq. (10), one can expand the vector potential at $t + \Delta t/2$ with a Taylor expansion in two ways as

$$\begin{aligned}
\vec{A}(t + \frac{\Delta t}{2}) &= \vec{A}(t) + \frac{\Delta t}{2}\dot{\vec{A}}(t) + \frac{\Delta t^2}{8}\ddot{\vec{A}}(t) + O(\Delta t^3) \\
\vec{A}(t + \frac{\Delta t}{2}) &= \vec{A}(t + \Delta t) - \frac{\Delta t}{2}\dot{\vec{A}}(t + \Delta t) + \frac{\Delta t^2}{8}\ddot{\vec{A}}(t + \Delta t) + O(\Delta t^3) \, .
\end{aligned} \tag{12}$$

Subtracting these two equations and dropping the $O(\Delta t^3)$ terms allows one to evaluate $A(t+\Delta t)$ using only one previous time step,

$$\vec{A}(t+\Delta t) \approx \vec{A}(t) + \frac{\Delta t}{2}\left[\dot{\vec{A}}(t) + \dot{\vec{A}}(t+\Delta t)\right] + \frac{\Delta t^2}{8}\left[\ddot{\vec{A}}(t) - \ddot{\vec{A}}(t+\Delta t)\right]. \tag{13}$$

Eq. (13) gives the vector potential with the desired $O(\Delta t^2)$ accuracy. We will use this expression in the RK4 algorithm for consistent formulation and easy implementation.

By combining the SRK4 and one of the equation for the evaluation of the vector potential, one obtains the approach summarized in Algorithm 3.

Algorithm 3 Simultaneous Runge-Kutta Method (4th order)

procedure SimultaneousRungeKutta1Step($n(\vec{r},t)$, $\{\psi_{ik}(\vec{r},t)\}$, $\vec{A}(t)$, $\dot{\vec{A}}(t)$) ▷ The initial condition

$c^{rk} \leftarrow \{1, \frac{1}{2}, \frac{1}{2}, 1\}$

for $m \leftarrow 1,2,3,4$ **do** ▷ Runge-Kutta stages

if $m = 1$ **then**

$\{\psi^{rk}_{ik}(\vec{r})\} \leftarrow \{\psi_{ik}(\vec{r},t)\}$

$\dot{\vec{A}}^{rk} \leftarrow \dot{\vec{A}}(t)$

else

$\{\psi^{rk}_{ik}(\vec{r})\} \leftarrow \{\psi_{ik}(\vec{r},t)\} + \Delta t\, c^{rk}_m\, \{k_{m-1}(\psi)\}$

$\dot{\vec{A}}^{rk} \leftarrow \dot{\vec{A}}(t) + \Delta t\, c^{rk}_m\, k_{m-1}(\dot{\vec{A}})$

end if

$\vec{J} \leftarrow$ ComputeCurrent($\{\psi^{rk}_{ik}(\vec{r})\}$)

$k_m(\dot{\vec{A}}) \leftarrow \dot{\vec{A}}(t) + \Delta t(-4\pi\vec{J})$

$\vec{A}^{rk} \leftarrow \vec{A}(t) + \Delta t \dot{\vec{A}}(t)$ ▷ can be replaced by Equation 10 or 13

$\{k_m(\psi)\} \leftarrow -iH\left[n(\vec{r},t), \vec{A}^{rk}\right]\{\psi^{rk}_{ik}(\vec{r})\}$

end for

$\{\psi_{ik}(\vec{r},t+\Delta t)\} \leftarrow \{\psi_{ik}(\vec{r},t)\} + \frac{\Delta t}{6}\left[\{k_1(\psi)\} + 2\{k_2(\psi)\} + 2\{k_3(\psi)\} + \{k_4(\psi)\}\right]$

$\dot{\vec{A}}(t+\Delta t) \leftarrow \dot{\vec{A}}(t) + \frac{1}{6}\left[k_1(\dot{\vec{A}}) + 2k_2(\dot{\vec{A}}) + 2k_3(\dot{\vec{A}}) + k_4(\dot{\vec{A}})\right]$

$\vec{J} \leftarrow$ ComputeCurrent($\{\psi_{ik}(\vec{r},t+\Delta t)\}$)

$\vec{A}(t+\Delta t) \leftarrow \vec{A}(t) + \Delta t \dot{\vec{A}}(t)$ ▷ can be replaced by Equation 10 or 13

$n(\vec{r},t+\Delta t) \leftarrow$ ComputeDensity($\{\psi_{ik}(\vec{r},t+\Delta t)\}$)

end procedure

Unlike the PC method, which only updates the vector potential once, there are multiple updates of the vector potential in the SRK4 algorithm. This results in a better approximation of the vector potential. As for the computational cost, the SRK4 approach requires only 4 applications of the Hamiltonian to each Kohn-Sham orbital per time step. In practice, we have found that the cost

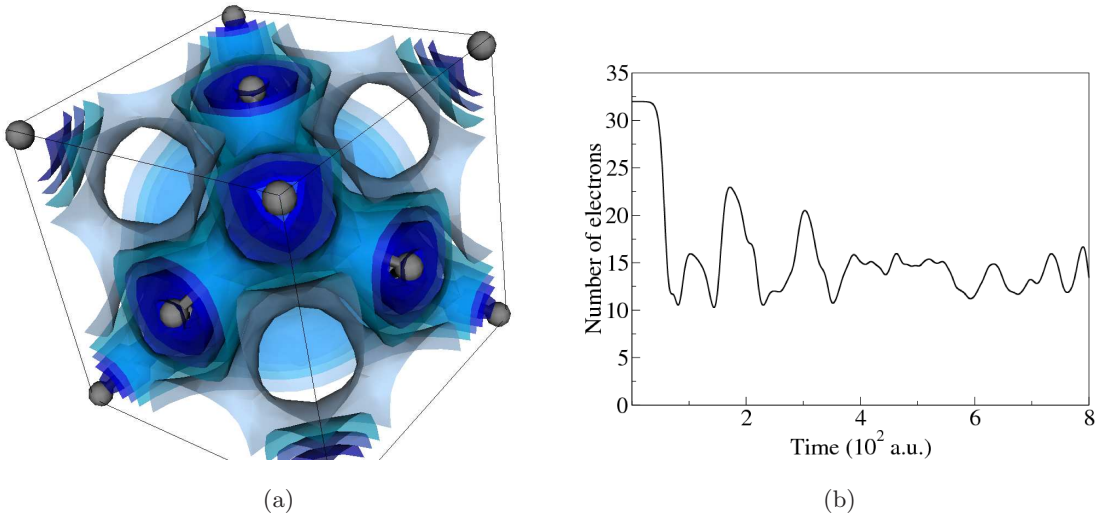

(a) (b)

FIG. 3. (Color online) (a) Ground state density iso-surface plot and (b) Number of electrons in the ground state orbitals as a function of time.

of the evaluation of the current in SRK4 is comparably expensive to these sparse matrix-vector multiplications, and include this cost in our algorithm analysis. We therefore find that the cost of SRK4 is only slightly lower than that of the PC method (see Table I) if the same time step is used. As we will show in the next section, the real advantage of the SRK4 method is that a time step of, Δt_{SRK4}=0.05 a.u. (0.0012 fs), gives well converged results. This time step is comparable to Δt_0=0.04 a.u., the maximum allowed time step for the Taylor propagation of the TDKS without coupling to the Maxwell-equations.

V. NUMERICAL EXAMPLES USING THE SRK4 METHOD

In this section we present numerical examples to show the computational efficiency and accuracy of the SRK4 approach. The system investigated is a diamond crystal perturbed by a delta-kick (as described in section II). There are 32 electrons per unit cell with 16 Kohn-Sham orbital doubly occupied for the ground state. The ground state density is shown in Fig. 3 (a) and a typical ground state population evolution in the excitation is shown in Fig. 3 (b).

In Fig. 4 we have compared the PC method with a time step of $\Delta t_{PC} = 0.02$ a.u. to SRK4 with a time step of, $\Delta t_{SRK4} = 0.05$ a.u. The Kohn-Sham orbitals are propagated for, T=400 a.u. The PC and SRK4 calculations are compared to a well converged benchmark Taylor propagation (Algorithm 1) with time step, $\Delta t_T = 0.002$ a.u. Over the course of the simulation errors in the PC method accumulate, leading the current, vector potential and energy to diverge compared to the

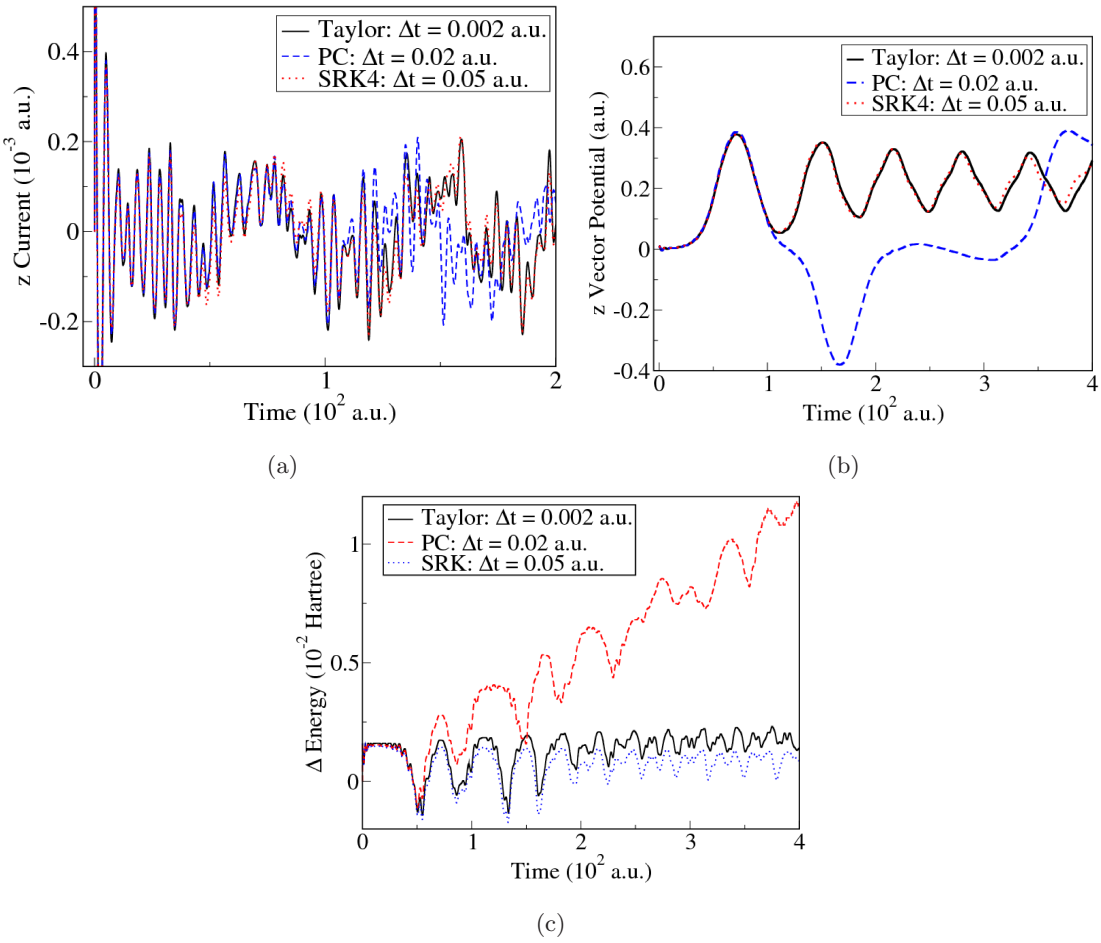

FIG. 4. (Color online) (a) Current, (b) vector potential and (c) total energy change of a diamond crystal after an applied delta kick on a $2 \times 2 \times 2$ k-point mesh. The system is propagated up to a time of 400 a.u. The current is only plotted up to 200 a.u. The PC and SRK4 propagation schemes are compared. $\Delta t_{PC} = 0.02$ a.u. is used for the PC method, in agreement with the previous sections. The results of the benchmark Taylor and PC methods, also shown in Fig. 2, are shown here for comparison. $\Delta t_{SRK4} = 0.05$ a.u. is used since it is the maximum allowed value for this scheme. The SRK4 method finds excellent agreement with the benchmark Taylor propagation with small time step, $\Delta t_T = 0.002$ a.u.

benchmark. The error of the energy accumulates at a very early time (about 50 a.u.). The SRK4 method remains stable and accurate for the whole duration.

This simple benchmark on a $2 \times 2 \times 2$ k-point mesh provides a quick test of the SRK4 algorithm. In practice, a more dense k-point mesh is required for comparison with experiments. In Fig. 5 we show the current and vector potential of a diamond crystal with a delta-kick perturbation on a $5 \times 5 \times 5$ k-point mesh for a total propagation time of 2000 a.u. The time steps for the Taylor benchmark and the SRK4 method are, as before, 0.002 a.u. and 0.05 a.u. respectively. We consider PC time steps of 0.02 a.u. and 0.05 a.u. On the denser k-point mesh the PC method

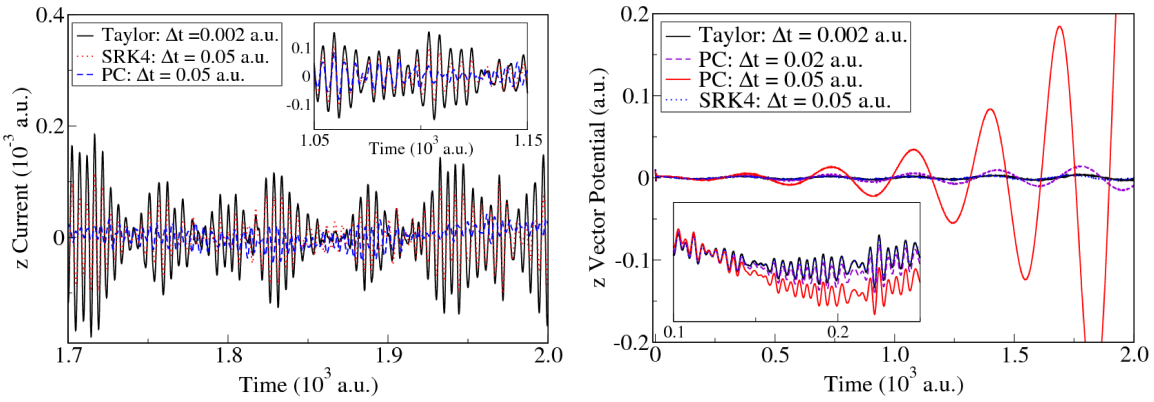

(a) (b)

FIG. 5. (Color online) (a) Current and (b) vector potential of a diamond crystal after an applied delta kick on a $5 \times 5 \times 5$ k-point mesh. The system is propagated up to a time of 2000 a.u. The current is plotted up from 1700 a.u. to 2000 a.u. Inset (a) shows the current in units of 10^{-3} a.u. from time 1050 a.u. to 1150 a.u. Inset (b) shows the z vector potential in a.u. from time 100 a.u. to 250 a.u. The PC and SRK4 propagation schemes are compared. Time steps of 0.02 a.u. and 0.05 a.u. are shown for the PC method. A time step of 0.05 a.u. is used for the SRK4 method. The SRK4 method finds excellent agreement with the benchmark Taylor propagation with small time step, $\Delta t_T = 0.002$ a.u. for the duration of the propagation.

remains relatively stable with a time step of 0.02 a.u. However, for a time step of 0.05 a.u. the vector potential calculated with the PC method becomes increasingly divergent (see Fig. 5.b). The current (Fig. 5.a) also diverges from the benchmark Taylor calculation. On the other hand the SRK4 method gives a more stable propagation with larger time steps than the PC method. The current calculated with SRK4 closely agrees with the benchmark, and the vector potential also shows excellent agreement.

In addition, the comparison between the simulations on $2 \times 2 \times 2$ k mesh and $5 \times 5 \times 5$ k mesh using Taylor propagation as benchmark indicates that there is almost no k point sampling dependency for the SRK4 method in applications, i.e. the SRK4 method matches the Taylor results in different k point sampling cases. The PC method shows better accuracy by increasing k point sampling from $2 \times 2 \times 2$ to $5 \times 5 \times 5$ (see Figs. 4 (a), (b) and Figs. 5 (a), (b)). By using more k points the disagreement (in current and vector potential) in case of PC method is delayed from 100 a.u. to about 1000 a.u.. The reason for this is probable the sensitivity of the PC approach to the smoothness of the density and potential, which requires more fine k point grid. In Ref. [24] a well converged result has been obtained by using $32 \times 32 \times 32$ k point mesh propagating the system up to 500 a.u. with a time step of 0.05 a.u.. A comparison of the PC and SRK4 methods for such a large k point mesh is computationally prohibitively expensive for the time duration needed (2000

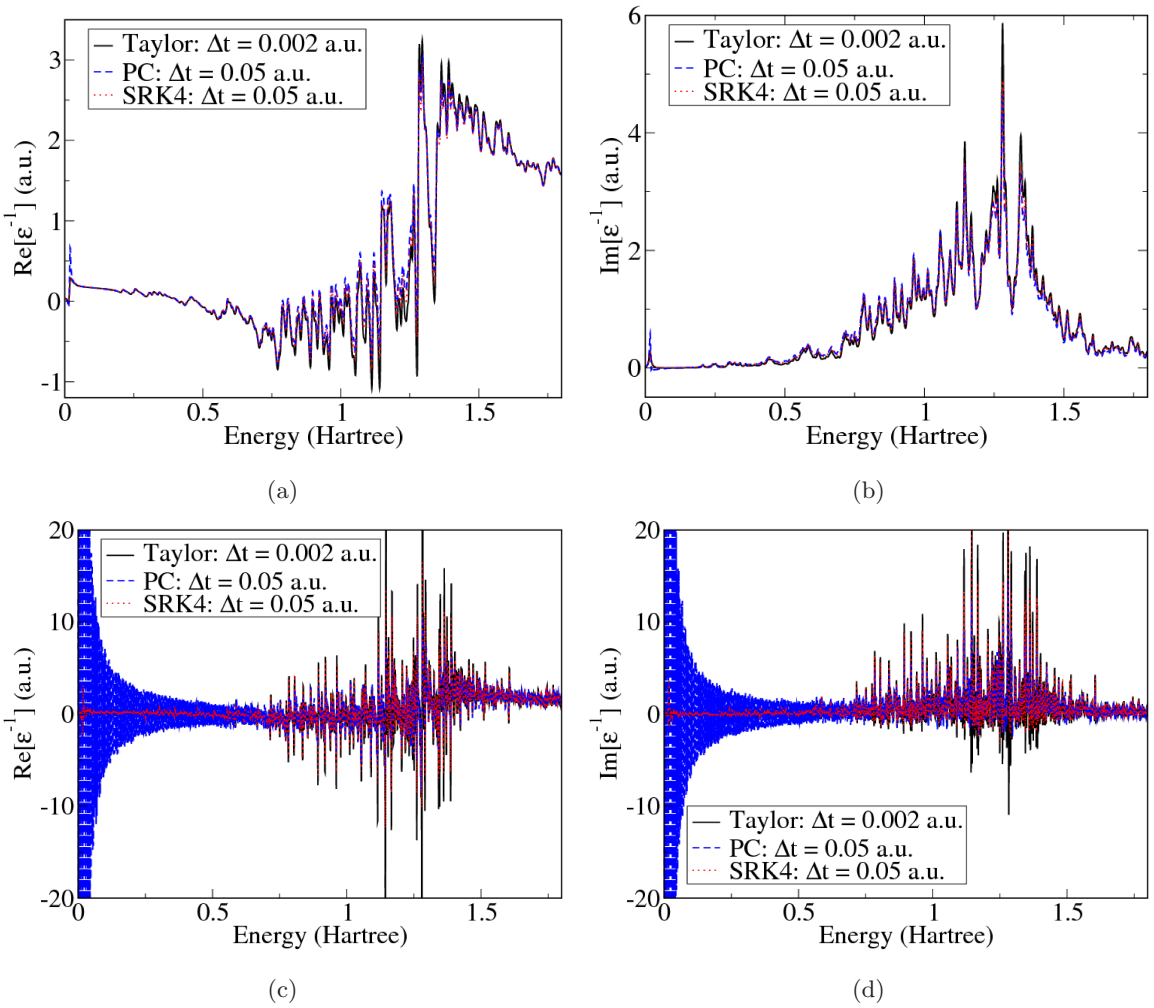

FIG. 6. (Color online) Inverse of the dielectric constant of a diamond crystal obtained through TDDFT simulations of the electron dynamics after a delta kick on a $5 \times 5 \times 5$ k-point mesh. The Kohn-Sham orbitals are propagated with the Taylor, PC, and SRK4 propagation schemes. Plots (a-b) show the (a) real and (b) imaginary parts of the inverse of the dielectric constant obtained by Fourier transforming the induced vector potential with a small broadening constant, $\eta = 0.005$ a.u. Plots (c-d) show the (c) real and (d) imaginary parts of the inverse of the dielectric constant obtained without a broadening parameter.

a.u). It is, however, quite likely (and our examples show) that the accuracy and allowable time step of the PC approach will increase with finer k point sampling.

To compare the different time propagation approaches further we calculate the dielectric function,

$$\frac{1}{\varepsilon(\omega)} = \frac{1}{A_0} \int_{0^+}^{\infty} dt\, e^{i\omega t - \eta t} \frac{\partial \vec{A}_{ind}(t) \cdot \vec{e}_z}{\partial t} + 1, \tag{14}$$

where η is a small broadening constant. Fig. 6 compares the dielectric functions calculated with the SRK4 and the PC methods, on a $5 \times 5 \times 5$ k-point mesh. The PC propagation with time

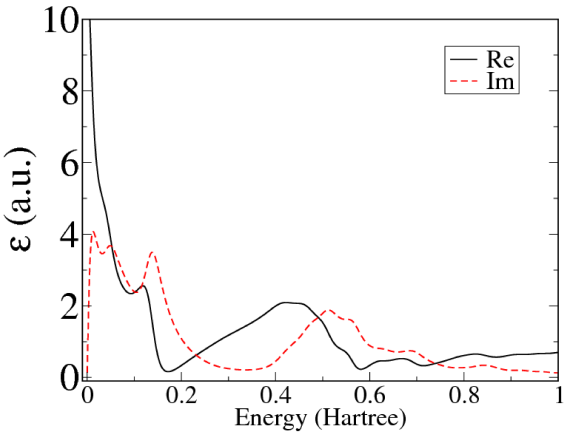

FIG. 7. (Color online) Real and imaginary components of the dielectric function of graphene obtained with TDDFT simulations of the electron dynamics after a delta kick on a $11 \times 19 \times 1$ k-point mesh. The Kohn-Sham orbitals are propagated with the SRK4 scheme with time step, 0.05 a.u.

step, $\Delta t = 0.05$ a.u., produces an unphysical plasmon peak as shown in Fig. 6 (a)-(b) in the low frequency range. This spurious plasmon peak has been observed in the literature [24], and has been associated with the use of discrete meshes in real and momentum spaces. The SRK4 and Taylor propagation produces a much smaller spurious plasmon peak, signifying the stability of the propagation.

To understand the qualitative difference observed in the spurious peaks of the two methods, we also calculated the dielectric constant without the broadening parameter, i.e. $\eta = 0$ a.u., as shown in Fig. 6 (c)-(d). The dielectric function, when calculated with the PC method and a time step of 0.05 a.u., contains a noisy tail at low energies due to the divergence of the vector potential. The amplitude of the noise is comparable to that of the dielectric function. The introduction of the broadening parameter averages this noise, yielding the small residual plasmon peak in Fig.6 (a)-(b). In contrast, the SRK4 method and benchmark Taylor calculation does not produce the unphysical noise at low energies. We note that reducing the time step of the PC method to 0.02 a.u. reduces the noise significantly.

Finally, to show the SRK4 method is a general solver for the Maxwell-TDKS equations, we provide two examples: First, a calculation for the dielectric function for graphene with an applied external field parallel to its plane. The k-point mesh used is $11 \times 19 \times 1$. Cheon et al. [45] calculated the dielectric function using linear response DFT with a fine k-point mesh. The dielectric function computed with SRK4 (see Fig. 7) agrees well with their results.

The second example is a simulation for an ultrafast laser pulse applied to the diamond crystal.

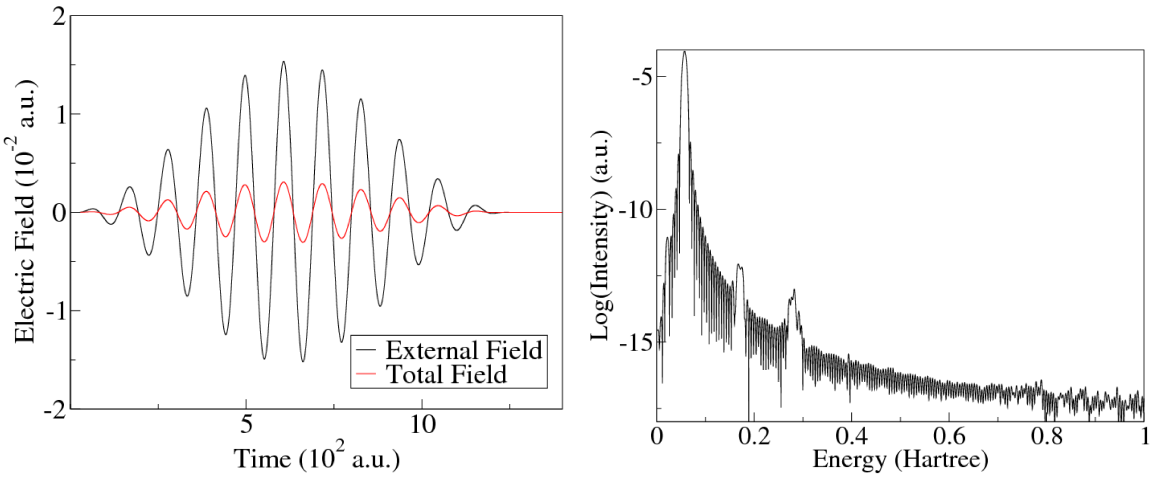

(a) (b)

FIG. 8. (Color online) (a) Electric field and current in diamond subject to a short laser pulse, calculated by the SRK4 method on a $12 \times 12 \times 12$ k-point mesh. The pulse is 1240 a.u. (30fs) wide with 0.057 a.u. (1.55eV) frequency and 0.0154 a.u. amplitude. (b) The first 3 harmonic generators located at 0.057 a.u., 0.171 a.u. and 0.285 a.u. as shown in the logarithmic scaled current transformed in energy space.

When the external field is applied, the induced field cancels part of the external field as shown in Fig. 8. The calculated current is Fourier transformed to find the high harmonic character of the signals [46]. After the transformation, we find 3 lowest harmonics at ω, 3ω and 5ω. The results agrees with the literature [46].

VI. SUMMARY

We have described an accurate method, the SRK4 approach, for time propagation of the coupled Maxwell and time-dependent Kohn-Sham equation. The new approach uses a simultaneous fourth-order Runge-Kutta based propagation of the vector potential and the Kohn-Sham orbitals. We have compared the approach to conventional fourth-order Taylor propagation and predictor-corrector methods. While the PC method was shown to have a divergence problem dependent on the time step, the SRK4 method can be used for long propagations without divergence. In our test case, the PC method with a time step of 0.02 a.u. gave reasonable results for a propagation time of 2000 a.u. However, even with this small time step increasing numerical inaccuracies in the vector potential were observed. The SRK4 method, in contrast, gave a more stable propagation with a larger time step of 0.05 a.u. . The SRK4 method has shown negligible dependence on k point sampling. Further test on different systems may help to explore the advantages and disadvantages

Summary of the simulations	Taylor	PC	SRK4
Time step (a.u.)	0.002	0.02*	0.05
Hamiltonian-Orbital Multiplication (operation cost A)	4	8	4
Current evaluation (operation cost B)	1	2	5
Total operation cost (A+0.8B)	4.8	9.6	8
Operations cost per a.u.	2400	480	160

* a time step for relatively stable PC propagation in this paper.

TABLE I. Comparison of 3 Maxwell-TDKS integrators: Taylor, PC and SRK4 methods.

of the present approach comparing to other schemes.

The computational efficiency of the three propagation schemes is summarized in Table I. Compared to the PC method with a time step of 0.02 a.u., the SRK4 method proves more computationally efficient by factor of 3. Since the PC method becomes more numerically unstable with increasing propagation times, one expects that an even shorter time step would be required. SRK4 remains very stable even for long propagation times, and therefore the SRK4 method becomes more advantageous as the propagation time is increased.

In energy space, the SRK4 method produced a better signal than the PC method. Fewer numerical artifacts were observed in the calculation of the dielectric function. One must use a broadening parameter for the PC method to remove a spurious plasmon peak at low energies. This artifact was much less prevalent in the SRK4 calculations, further highlighting the numerical stability of this method.

In the present work we have tested the Coupled Maxwell and Kohn-Sham propagation for crystalline materials. In the future it would be interesting to explore the possibility of the application for molecules, gases or liquids. Another area of interest is the investigation of the cases with weaker laser and soft bonds [47].

Due to its greater computational efficiency, numerical stability, and more rigorous foundation as a differential equation solver, we recommend the SRK4 method for the solution of the Maxwell-TDKS equations in further studies of coupled Schrödinger-Maxwell.

ACKNOWLEDGMENTS

This work has been supported by the National Science Foundation (grant) PHY-1314463. This work used the Extreme Science and Engineering Discovery Environment (XSEDE), which is supported by National Science Foundation and resources of the National Energy Research Scientific

Computing Center, a DOE Office of Science User Facility supported by the Office of Science of the U.S. Department of Energy under Group ID 46319.

[1] Schultze Martin, Bothschafter Elisabeth M., Sommer Annkatrin, Holzner Simon, Schweinberger Wolfgang, Fiess Markus, Hofstetter Michael, Kienberger Reinhard, Apalkov Vadym, Yakovlev Vladislav S., Stockman Mark I., and Krausz Ferenc, Nature **493**, 75 (2013), 10.1038/nature11720.

[2] A. V. Mitrofanov, A. J. Verhoef, E. E. Serebryannikov, J. Lumeau, L. Glebov, A. M. Zheltikov, and A. Baltuška, Phys. Rev. Lett. **106**, 147401 (2011).

[3] Ghimire Shambhu, DiChiara Anthony D., Sistrunk Emily, Agostini Pierre, DiMauro Louis F., and Reis David A., Nat Phys **7**, 138 (2011), 10.1038/nphys1847.

[4] Hohenleutner M., Langer F., Schubert O., Knorr M., Huttner U., Koch S. W., Kira M., and Huber R., Nature **523**, 572 (2015).

[5] Neppl S., Ernstorfer R., Cavalieri A. L., Lemell C., Wachter G., Magerl E., Bothschafter E. M., Jobst M., Hofstetter M., Kleineberg U., Barth J. V., Menzel D., Burgdorfer J., Feulner P., Krausz F., and Kienberger R., Nature **517**, 342 (2015).

[6] E. Weinan, J. Lu, and X. Yang, Acta Mathematica Sinica, English Series **27**, 339 (2011).

[7] M. Šindelka, Phys. Rev. A **81**, 033833 (2010).

[8] Lorin E., Chelkowski S., and Bandrauk A., Computer Physics Communications **177**, 908 (2007).

[9] E. Runge and E. K. U. Gross, Phys. Rev. Lett. **52**, 997 (1984).

[10] C. A. Ullrich, *Time-dependent density-functional theory: concepts and applications* (Oxford University Press: Oxford, UK, 2012).

[11] O. Keller, Physics Reports **268**, 85 (1996).

[12] G. Bao, D. Liu, and S. Luo, SIAM Journal on Applied Mathematics **73**, 741 (2013), http://dx.doi.org/10.1137/12087147X.

[13] N. T. Maitra, I. Souza, and K. Burke, Phys. Rev. B **68**, 045109 (2003).

[14] C. Pellegrini, J. Flick, I. V. Tokatly, H. Appel, and A. Rubio, Phys. Rev. Lett. **115**, 093001 (2015).

[15] Y. Gao and D. Neuhauser, The Journal of Chemical Physics **137**, 074113 (2012), 10.1063/1.4745847.

[16] M. Farzanehpour and I. V. Tokatly, Phys. Rev. B **90**, 195149 (2014).

[17] M. Ruggenthaler, J. Flick, C. Pellegrini, H. Appel, I. V. Tokatly, and A. Rubio, Phys. Rev. A **90**, 012508 (2014).

[18] M. Ruggenthaler, F. Mackenroth, and D. Bauer, Phys. Rev. A **84**, 042107 (2011).

[19] I. Ahmed, E. H. Khoo, E. Li, and R. Mittra, Antennas and Wireless Propagation Letters, IEEE **9**, 914 (2010).

[20] I. V. Tokatly, Phys. Rev. Lett. **110**, 233001 (2013).

[21] T. Takeuchi, S. Ohnuki, and T. Sako, Phys. Rev. A **91**, 033401 (2015).

[22] G. Vignale and M. Rasolt, Phys. Rev. Lett. **59**, 2360 (1987).

[23] K. Yabana, T. Sugiyama, Y. Shinohara, T. Otobe, and G. F. Bertsch, Phys. Rev. B **85**, 045134 (2012).

[24] G. F. Bertsch, J.-I. Iwata, A. Rubio, and K. Yabana, Physical Review B **62**, 7998 (2000).

[25] G. Wachter, C. Lemell, J. Burgdörfer, S. A. Sato, X.-M. Tong, and K. Yabana, Physical Review Letters **113** (2014), 10.1103/physrevlett.113.087401.

[26] S. A. Sato, Y. Taniguchi, Y. Shinohara, and K. Yabana, The Journal of Chemical Physics **143**, 224116 (2015), 10.1063/1.4937379.

[27] S. A. Sato, Y. Shinohara, T. Otobe, and K. Yabana, Phys. Rev. B **90**, 174303 (2014).

[28] N. Troullier and J. L. Martins, Phys. Rev. B **43**, 1993 (1991).

[29] J. P. Perdew and A. Zunger, Phys. Rev. B **23**, 5048 (1981).

[30] J. R. Chelikowsky, N. Troullier, and Y. Saad, Phys. Rev. Lett. **72**, 1240 (1994).

[31] E. L. Briggs, D. J. Sullivan, and J. Bernholc, Phys. Rev. B **54**, 14362 (1996).

[32] J. A. Driscoll, S. Bubin, W. R. French, and K. Varga, Nanotechnology **22**, 285702 (2011).

[33] J. A. Driscoll, S. Bubin, and K. Varga, Phys. Rev. B **83**, 233405 (2011).

[34] J. A. Driscoll, B. Cook, S. Bubin, and K. Varga, J. Appl. Phys. **110**, 024304 (2011).

[35] J. A. Driscoll and K. Varga, Phys. Rev. B **80**, 245431 (2009).

[36] S. Bubin, M. Atkinson, K. Varga, X. Xie, S. Roither, D. Kartashov, A. Baltuška, and M. Kitzler, Phys. Rev. A **86**, 043407 (2012).

[37] S. Bubin and K. Varga, Appl. Phys. Lett. **98**, 154101 (2011).

[38] S. Bubin and K. Varga, J. Appl. Phys. **110**, 064905 (2011).

[39] S. Bubin and K. Varga, Phys. Rev. B **85**, 205441 (2012).

[40] S. Bubin, B. Wang, S. Pantelides, and K. Varga, Phys. Rev. B **85**, 235435 (2012).

[41] A. Russakoff, S. Bubin, X. Xie, S. Erattupuzha, M. Kitzler, and K. Varga, Phys. Rev. A **91**, 023422 (2015).

[42] A. Russakoff and K. Varga, Phys. Rev. A **92**, 053413 (2015).

[43] K. Yabana, T. Nakatsukasa, J.-I. Iwata, and G. F. Bertsch, phys. stat. sol. (b) **243**, 1121 (2006).

[44] W. H. Press, S. A. Teukolsky, W. T. Vetterling, and B. P. Flannery, *Numerical Recipes in FORTRAN; The Art of Scientific Computing*, 2nd ed. (Cambridge University Press, New York, NY, USA, 1993).

[45] S. Cheon, K. D. Kihm, H. g. Kim, G. Lim, J. S. Park, and J. S. Lee, Scientific Reports **4**, 6364 (2014).

[46] T. Otobe. First-principle description for the high-harmonic generation in a diamond by intense short laser pulse. *Org. Biomol. Chem.* **2012**, *111*, 093112.

[47] M. Ben-Nun, J. Quenneville, , and T. J. Martnez*, The Journal of Physical Chemistry A **104**, 5161 (2000), http://dx.doi.org/10.1021/jp994174i

.